doi:10.3788/gzxb20144306.0625002

指数掺杂GaAs阴极光子增强热电子发射型太阳能转换器转化效率理论计算

唐伟东[1,2],杨文正[1],杨阳[1],孙传东[1],蔡志鹏[1,2]
(1 中国科学院西安光学精密机械研究所 瞬态光学与光子技术国家重点实验室,西安 710119)
(2 中国科学院大学,北京 100049)

摘 要:光子增强热电子发射型太阳能转换器是一种理论效率极高的新型太阳能利用技术.提出利用指数掺杂GaAs材料作为光子增强热电子发射型太阳能转换器阴极,基于能量守恒及电子扩散漂移发射模型,理论计算了指数掺杂GaAs阴极光子增强热电子发射型太阳能转化器的转化效率.结果表明:指数掺杂GaAs可以显著提高光子增强热电子发射效率;指数掺杂GaAs光子增强热电子太阳能转化器转化效率随聚光倍数的增加和阴极表面电子复合速率减小而单调上升;当太阳基数大于200、阴极表面复合小于10^4 cm/s时,指数掺杂GaAs阴极光子增强热电子发射型太阳能转换器效率可达30%.

关键词:PETE;太阳能转化器;指数掺杂;GaAs阴极;转化效率
中图分类号:TK514;O462.1 **文献标识码**:A **文章编号**:1004-4213(2014)06-0625002-6

Conversion Efficiency of Photon Enhanced Thermionic Emission Solar Converters with Exponential Doping GaAs Cathodes

TANG Wei-Dong[1,2], YANG Wen-Zheng[1], YANG Yang[1,2], SUN Chuan-Dong[1], CAI Zhi-Peng[1,2]
(1 *State Key Laboratory of Transient Optics and Photonics, Xi'an Institute of Optics and Precision Mechanics, Chinese Academy of Sciences, Xi'an* 710119 *China*)
(2 *University of Chinese Academy of Sciences, Beijing* 100049, *China*)

Abstract: Photon-enhanced thermionic emission solar energy converter is a new highly efficient solar energy utilization technologies. An exponential doping GaAs material was presented as the cathode of photon-enhanced thermionic emission solar converter. The conversion efficiencies of the photon-enhanced thermionic emission solar devices with exponential doping GaAs were theoretically analyzed by using the energy-balance and diffusion-drift-emission models. The results show that exponential doping GaAs prominently enhances photon-enhanced thermionic emission conversion, and the efficiency of photon-enhanced thermionic emission solar converters with exponential doping GaAs cathodes is a monotonically increasing function of sun concentration and a monotonically decreasing function of cathode surface recombination velocities. The efficiency of the converter can reach 30% at a flux concentration larger than 200 suns and surface recombination velocities maintained at fewer than 10^4 cm/s.

Key words: PETE; Solar converter; Exponential doping; GaAs cathode; Conversion efficiency
OCIS Codes: 250.1500; 250.5230; 250.6715

Foundation item: The Knowledge Innovation Project of Chinese Academy of Sciences (No. KGCX2-YW-399+10) and the West Light Foundation of Chinese Academy of Sciences
First author: TANG Wei-dong (1986-), male, Ph. D candidate, mainly focuses on photovoltaic and photothermal solar cell. Email: tangwd@opt.ac.cn.
Corresponding author: YANG Wen-zheng (1975-), female, associate professor, Ph. D. degree, mainly focuses on semiconductor optoelectronic devices. Email: ywz@opt.ac.cn.
Received: Oct.12, 2013; **Accepted**: Dec.5, 2013

0 Introduction

Photon-Enhanced Thermionic Emission (PETE)[1], which combines photovoltaic and thermionic effects into a single physical process to utilize the high per-quanta energy of photons and the available thermal energy caused by thermalization and absorption losses, is an appealing technology for converting solar energy. A PETE solar converter has the same vacuum-gap parallel-plate architecture as a thermionic converter[2-3], consisting of a p-type semiconductor as the cathode that receives solar light and heat from a solar concentrator, an n-type semiconductor or a metal as the anode that collects electrons and disposes of waste heat to power a secondary thermal system, a vacuum gap between the two electrodes that restrains the temperature of the anode. PETE conversion potentially has higher efficiency than conventional photovoltaic conversion because it can extract electricity from solar radiation and express it as thermal energy. Heat extracted from the anode can then be used to generate additional electricity. SCHWEDE[1] and SEGEV *et al*[4]. both presented estimates of conversion efficiency that are significantly higher than those of conventional thermionic emission, i. e., an efficiency exceeding 40% for an incident solar radiation concentration of 1 000 and a temperature below 1 000 ℃.

GaN material was utilized as PETE cathode to demonstrate the PETE mechanism in Ref. [1]. However, with the wide band gap of 3.3 eV, only 1% of solar photons have energies exceeding the GaN band gap, making GaN not well suited for PETE solar applications. For a PETE solar device to work effectively, the semiconductor cathode requires a suitable band-gap energy that matches the energy of solar photons, i. e., within the range of 1.1 eV to 1.7 eV[1]. VARPULA and PRUNNILA[5] calculated the efficiency of PETE devices with Si material of 1.1 eV according to a diffusion-emission model. Relevant semiconductor effects, such as diffusion and surface recombination, presented negative effects on PETE conversion, which could reduce efficiency to below 15%.

A GaAs material of 1.42 eV is a promising candidate for PETE cathodes; such material exhibits enormous performance advantages in solar energy utilization[6-9]. A large number of investigations of GaAs applications in vacuum imaging and as electron sources have shown that GaAs cathodes have a prominent photoemission feature and varied doping structures that result in notable enhancements on its emission[10-17]. However, in previous PETE analyses, the PETE GaAs cathodes and the effect of its doping method on the conversion efficiency of PETE devices have not been addressed.

In the present study, we propose an exponential doping GaAs cathode as a solar converter and consider its PETE according to the energy-balance and diffusion-drift-emission models. Unlike in previous configurations, the cathode is not assumed as thermally isolated and consisting of two sections, i. e., the substrate and the GaAs film, in our cathode thermal balance model. The substrate works as an infrared absorber to gather sub-band-gap photon energy, and the film is expected to absorb all above-band-gap energy photons and emit electrons efficiently. A coupled thermal and electrical energy balance is provided to illustrate the temperature of the two sections as a function of the input flux concentration. In the PETE conversion model presented in Ref. [1], only a single rate equation was used to describe the surface emission of the PETE cathode, thus neglecting numerous important effects in semiconductors. In the proposed diffusion-drift- emission model, relevant effects such as diffusion and drift of "hot electron," excess carrier lifetime, bulk and surface recombination, and photon absorption are considered for PETE conversion.

1 Analysis model

1.1 The energy-balance model

A complete thermal and electrical energy model of a PETE device consists of a network of thermally linked masses selected to capture essential system components, as shown in Fig. 1. Solar radiation is absorbed by the cathode, and then, the cathode emits blackbody radiation and electron current J_C toward the anode. Meanwhile, the anode releases blackbody radiation and reverses thermionic current J_A. A Phase-Change Material (PCM) is incorporated into the model to limit the anode temperature from restraining its reverse energy. The excess heat energy from the anode

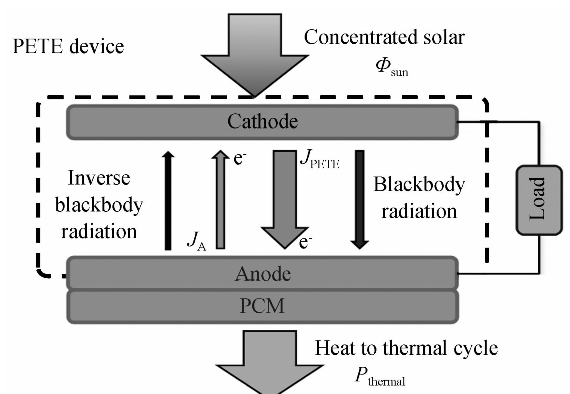

Fig. 1 The thermal and electrical energy model of the PETE device

can then be used to power a secondary thermal system. The surface thermal convection and radiation of the device are also considered. The cathode sub-assembly can be divided into two components, i. e. , an infrared absorber substrate and a GaAs film cathode, as shown in Fig. 2. The sub-band gap solar power is assumed to increase the temperature of the substrate through thermal coupling, and the film cathode absorbs the above-band-gap photon.

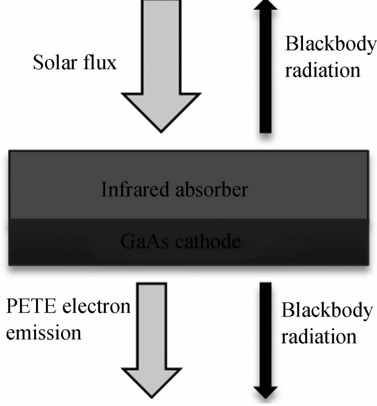

Fig. 2 The energy-balance model of the cathode

The energy-balance model of the cathode is shown in Fig. 2. A couple of 1D energy equations expressed as time differences are given as

$$m_s C_{p,s}\frac{dT_s}{dt}=\beta_s M\Phi_{sun,hv<E_g}-G_{s,amb}(T_s-T_{s,amb})-\varepsilon_s\delta(T_s^4-T_{sky}^4)-G_{s,c}(T_s-T_c) \quad (1)$$

$$m_c C_{p,c}\frac{dT_c}{dt}=(1-R_c)(1-e^{-\alpha H_c})M\left[\Phi_{sun,hv>E_g}-n_{hv>E_g}\left(E_g+\frac{3}{2}kT_c\right)\right]-G_{c,amb}(T_c-T_{c,amb})-\varepsilon_c\delta(T_c^4-\varepsilon_a T_a^4)-G_{c,s}(T_c-T_s) \quad (2)$$

using subscripts s for substrate, c for cathode, a for anode, amb for ambient air, sky for sky, and sun for sunlight; and where m is the mass, C is the heat capacity, T is the temperature, β is the absorptance, M is the concentration, Φ is the solar flux, hv is the photon energy, E_g is the band gap, G is the thermal conductance, ε is the emissivity, and R is the reflectance of the cathode. For the absorption coefficient α of GaAs, we employ a widely used semi-empirical model.

1.2 The diffusion-drift-emission model

PETE current density is defined as follows

$$J_C=A_C^* T_C^2\exp\left(-\frac{\phi_C-(E_{F,n}-E_F)}{kT_C}\right) \quad (3)$$

where $A_C^*=4\pi qm^* k^2/h^3$ is the cathode Richardson constant; T_C is the cathode emission temperature; ϕ_C is the work function of the cathode; and the quasi-Fermi level $E_{F,n}=E_F+kT_C\ln(n/n_{eq})$, where E_F is the Fermi level, n is the total electron concentration in the conduction band, and n_{eq} is the equilibrium concentration without photoexcitation. The PETE current density expression can be simplified in the form of electron density, as follows

$$J_C=A_C^* T_C^2\exp\left(-\frac{\phi_C}{kT_C}\right)\frac{n}{n_{eq}} \quad (4)$$

Electron density n can be calculated using the continuity equation, the generation and recombination rate equations, and the drift-diffusion current equations for the charge carriers. We assume that the band bending near the cathode surface is neglected because the effect is minimal and the PETE device is mostly operated near the flat-band case, where band bending disappears. The excess electron density $\Delta n(x)=n(x)-n_{eq}$ can be described as

$$\frac{d^2\Delta n(x)}{dx^2}-\frac{\mu_n|E|}{D_n}\frac{d\Delta n(x)}{dx}+\frac{g(x)}{D_n}-\frac{\Delta n(x)}{D_n\tau_n}=0 \quad (5)$$

where D_n is the diffusion coefficient, μ_n is the mobility, E is the built-in field formed by exponential doping, and $g(x)$ is the carrier generated by the solar photon that is expressed as

$$g(x)=\int_{E>E_g}(1-R(\lambda))\Phi_{sun,hv>E_g}(\lambda)\alpha(\lambda)\cdot\exp(-\alpha(\lambda)x)d\lambda \quad (6)$$

where λ is the wavelength of the solar photon with an energy greater than that of the band gap. For simplicity, the $g(x)$ of the GaAs that responds to the AM1.5 direct+circumsolar is fitted as

$$g(x)=(1-R)\Phi\alpha\exp(-\alpha\cdot x) \quad (7)$$

where $\Phi=1.9\times10^{17}\ \mathrm{cm^2/s}$, $\alpha=2\times10^4\ \mathrm{cm^{-1}}$, and $R=0.25$. The boundary conditions are

$$\left[D_n\frac{d\Delta n(x)}{dx}-\mu|E|\Delta n(x)\right]\Bigg|_{x=0}=S_v\Delta n(0) \quad (8)$$

$$\left[D_n\frac{d\Delta n(x)}{dx}-\mu|E|\Delta n(x)\right]\Bigg|_{x=H}=-\frac{A_C^* T_C^2}{q}\cdot\exp\left(-\frac{\phi_C}{kT_C}\right)\left(1+\frac{\Delta n(H)}{n_{eq}}\right)-S_c\Delta n(H) \quad (9)$$

where H is the thickness of the cathode emission layer; and S_v and S_c are the front and back surface recombination velocities, respectively.

The excess electron density of the exponential doping GaAs cathode can be deduced from the preceding continuity equation with boundary conditions. The equation of PETE current density according to the diffusion-drift-emission model is given by

$$J_C=J_T\left(1+\left(\Delta n_{sun}-\frac{L_{ED}M}{qD_n}J_T\right)\left(n_{eq}+\frac{L_{ED}M}{qD_n}J_T\right)^{-1}\right) \quad (10)$$

where

$$J_T=A_C^* T_C^2\exp\left(-\frac{\phi_C}{kT_C}\right)$$

$$M=\frac{1}{Q}\left[\cosh\left(\frac{H}{L_{ED}}\right)+\frac{L_{ED}S_v}{D_n}\sinh\left(\frac{H}{L_{ED}}\right)\right]$$

$$Q=\sinh\left(\frac{H}{L_{ED}}\right)+\frac{L_{ED}S_v}{D_n}\cosh\left(\frac{H}{L_{ED}}\right)+U\frac{L_{ED}S_c}{D_n}$$

$$U=\cosh\left(\frac{H}{L_{\mathrm{ED}}}\right)+\frac{L_{\mathrm{ED}}S_{\mathrm{v}}}{D_n}\sinh\left(\frac{H}{L_{\mathrm{ED}}}\right)$$

$$\Delta n_{\mathrm{sun}}=\frac{\tau_n\alpha\Phi(1-R)}{1-\alpha^2L_{\mathrm{ED}}^2}\left\{\mathrm{e}^{-\alpha H}-\frac{L_{\mathrm{ED}}}{Q}\left[\frac{S_{\mathrm{v}}}{D_n}+\alpha+\mathrm{e}^{-\alpha H}U\left(\frac{S_{\mathrm{c}}}{D_n}-\alpha\right)\right]\right\}$$

$$L_{\mathrm{ED}}=\frac{L_{\mathrm{E}}+\sqrt{L_{\mathrm{E}}^2+4L_{\mathrm{D}}^2}}{2}$$

where L_{ED} is the electron diffusion and drift length; $L_E=\mu_n\tau_nE$ is the electron drift length that represents the drift distance of electrons within the lifetime τ_n as a result of the built-in electric field E; $L_{\mathrm{D}}=\sqrt{D_n\tau_n}$ is the diffusion length of electrons; and Δn_{sun} represents the excess electrons resulting from photoexcitation.

2 Results and discussion

2.1 Cathode temperature

A function of the cathode temperature with sun concentration can be obtained under steady-state conditions, wherein the temperature difference with time is zero, as $\mathrm{d}T_{\mathrm{s}}/\mathrm{d}t=0$, $\mathrm{d}T_{\mathrm{c}}/\mathrm{d}t=0$. The gap between the cathode and the anode is a vacuum, thus, $G_{\mathrm{c,camb}}=0$. The thickness of the cathode H_{c} is negligible compared with that of the absorber H_{s}; hence, we assume that the temperature of the cathode across the thickness direction is uniform and equal to the bottom temperature of the cathode. The temperature of the anode T_{A} is set to 300 ℃ to allow the heat engine that is potentially coupled with the anode to have a reasonably high efficiency, where $\delta=5.67\times10^{-8}$ W·m^{-2}·K^{-4}, and $\varepsilon=1$ is assumed for simplicity. Ambient temperature $T_{\mathrm{s,amb}}=25$ ℃. The band gap of GaAs is 1.42 eV. For the AM1.5 direct+circumsolar spectrum, the sub-band-gap photon energy $\Phi_{\mathrm{sun},h\nu<E_{\mathrm{g}}}=340$ W·m^{-2}·s^{-1}, the above-band-gap energy $\Phi_{\mathrm{sun},h\nu>E_{\mathrm{g}}}=660$ W·m^{-2}·s^{-1}, and its photons $n_{h\nu>E_{\mathrm{g}}}=1.9\times10^{21}$ m^{-2}·s^{-1}. The thermal convection of air with the absorber surface $G_{\mathrm{s,amb}}=12$ W·m·K, where $G_{\mathrm{s,c}}$ is the thermal conductance of the interface between the cathode and the absorber. The thickness of the GaAs cathode is negligible compared with that of the substrate $G_{\mathrm{s,c}}=1.3/H_{\mathrm{s}}=(1.3\div3)$ W·m^{-1}·K, where $H_{\mathrm{s}}=3$ mm is the thickness of the substrate.

The cathode emission surface temperature T_{c} is shown as a function of sun concentration M in Fig. 3, where the solid curve is the idealized absorption, $\beta=1$ indicates that all sub-band-gap solar energy is absorbed, and $R=0$ denotes the sum reflectance of the cathode and the substrate for above-band-gap photons. At low concentrations, the solar thermal power and the excess photon energy above the band gap, which are converted into thermal energy by thermalization, are insufficient to maintain the anode at a temperature of 500 K. Hence, the low concentration of $M<50$ suns is not the focus of our investigation. As concentration increases, the temperature also increases and eventually forms a linear incensement with the concentration. A temperature of 1 000 °C can be achieved at $M=500$ suns for an idealized cathode. However, the thermal absorptance of the cathode substrate and the optics reflectance of the GaAs cathode are not idealized practically. The surface temperature of the PETE cathode with a modified solar absorption is lower than those of the idealized conditions. Moreover, achieving the same temperatures requires a sun concentration that may be difficult to attain in practical implementations.

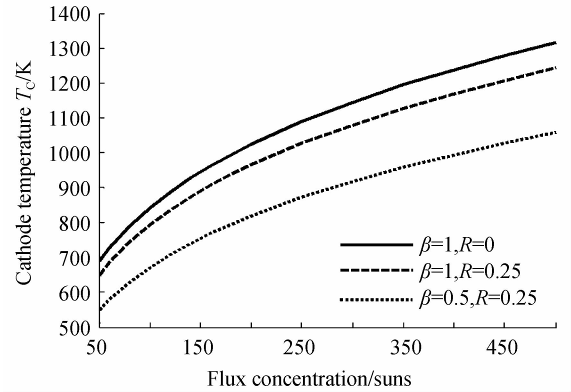

Fig. 3 Cathode temperature increasing with flux concentration

2.2 PETE cathode quantum efficiency

The built-in electric field E formed by the exponential doping structure is equal to $\beta kT_{\mathrm{C}}/qH$, where β is the exponential doping coefficient and is given as $\ln(N_0/N_{\mathrm{H}})/H$ (where N_0 and N_{H} are the initial and end doping concentrations of the GaAs film, respectively). We assume the following cathode parameters: $D_n=120$ cm^2/s, $\mu_n=4\ 800$ cm^2/V·s, $H=2$ μm, $S_{\mathrm{v}}=10^4$ cm/s, $S_{\mathrm{c}}=10^4$ cm/s, and $\tau_n=10$ ns. The cathode electron affinity χ is 0.6 eV, and $\phi_{\mathrm{C}}=2.02$ eV, which varies as temperature is neglected.

Fig. 4 shows the PETE quantum efficiency, i.e., the emitted electron above the band-gap photon, as a function of the temperature for cathode end-doping concentrations of 10^{19}, 5×10^{18}, 1×10^{18}, 5×10^{17}, and 10^{17} cm^{-3}, with the same initial doping concentration of 10^{19} cm^{-3}. A significant increase in quantum efficiency with the exponential doping cathode gradient that is in contrast to the emission efficiency of the uniform cathode is shown in Fig. 4. A cathode doping concentration that exponentially ranges from 1×10^{19} cm^{-3} to 1×10^{17} cm^{-3} can form a stronger built-in field and has better emission efficiency than the other four cathodes. However, such concentration requires a

more complicated doping structure that may be difficult in practical implementations. Hence, choose the exponential doping GaAs cathode with a gradient of 1×10^{19} cm^{-3} to 1×10^{18} cm^{-3} for the PETE device.

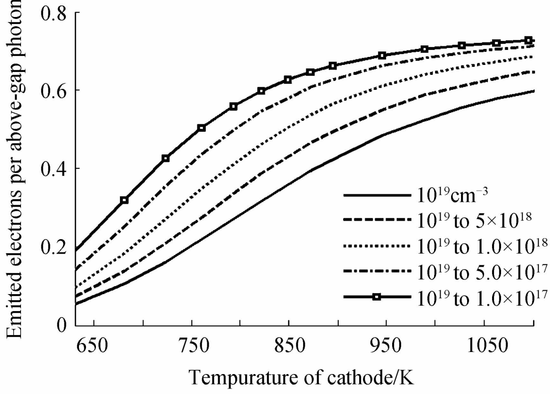

Fig. 4 The PETE quantum efficiency of the GaAs cathodes with various doping gradients as a function of temperature

2.3 Conversion efficiency of the PETE device

The idealized power output of a PETE device is denoted by the difference between the cathode current J_C and the reverse thermionic current from the anode, multiplied by the difference between the cathode and the anode work functions:

$$P_{PETE}=(J_C-J_A)(\phi_C-\phi_A) \quad (11)$$

Fig. 5 shows the PETE conversion efficiency as a function of the flux concentration of exponential and uniform GaAs cathodes with material parameters $\phi_A=0.9$ eV and $A_A^*=57.6$ A/cm^2/K^2. Compared with the PETE conversion efficiency curve of the uniform cathode, the device equipped with the exponential doping GaAs cathode exhibits better PETE conversion capability. Exponential efficiency rapidly increases to 30%, with the concentration of $M<150$ suns in the low region, where the most obvious enhancement by the exponential structure occurs. As temperature increases, PETE conversion also gradually increases and eventually reaches an efficiency plateau of 32%. This result indicates that the optimization concentration is $M=200$ suns, with a conversion efficiency of 30%. The effect of surface recombination on the efficiency of the PETE device is shown in Fig. 6. Conversion efficiency can be reduced by increasing the recombination velocities S_v and S_c. Compared with the front recombination velocity S_v, efficiency is more sensitive to the back emission surface recombination velocity S_c. Although photogeneration is significantly stronger near the front surface than near the back surface, most photoelectrons are drawn toward the emission surface by the field force. Fig. 6 also shows that $S_v<10^5$ cm/s and $S_c<10^4$ cm/s are essential for a realistic PETE device.

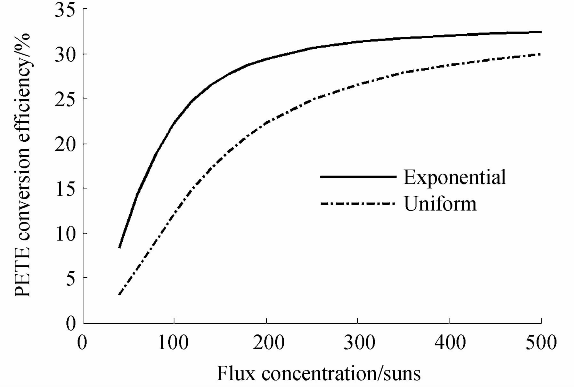

Fig. 5 Efficiencies of PETE devices with exponential and uniform doping cathodes as functions of flux concentration and with phosphorus-doped diamonds as anodes

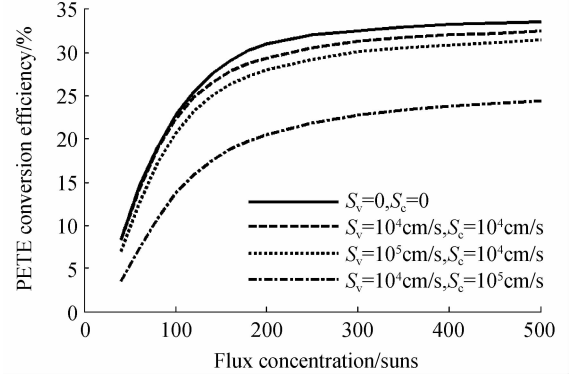

Fig. 6 Conversion efficiency of an exponential doping GaAs device with various surface recombination velocities S_v and S_c

3 Conclusion

A GaAs material embedded with an exponential doping structure is proposed for PETE solar converters. The cathode operating temperature, as a function of the incident radiation flux, is solved by the coupling between electrical and thermal energy balances. A diffusion-drift-emission theoretical model is presented for PETE. In contrast to the result for a uniform doping GaAs material, exponential doping GaAs exhibits a prominent emission enhancement on PETE, which significantly increases conversion efficiency. The conversion efficiency with an exponential GaAs cathode increases rapidly with sun concentration, and an efficiency of 30% is achieved at a flux concentration of 200 suns and a temperature of 900 K. Such efficiency may be further improved by using nanostructures[18-20], reducing the reflection coefficient, and increasing light absorption. The calculated efficiency is slightly lower than the theoretical limits of single-junction photovoltaic cells. Nevertheless, the PETE device exhibits natural thermal coupling with a thermal engine, which overcomes operating

temperature discrepancy along with photovoltaic and thermal engines. The energy coupled with the thermal engine through the anode, which is not considered in the present study, should also be managed. Full optimization of tandem efficiency will be considered in future studies.

References

[1] SCHWEDE J W, BARGATIN I, RILEY D C, *et al*. Photon-enhanced thermionic emission for solar concentrator systems [J]. *Nature Materials*, 2010, **9**(1): 762-767.

[2] JULIAN GOLDSMID H. Thermionic energy conversion[J] *Springer Series in Materials Science*, 2009, **121**(1):221-233.

[3] HATSOPOULOS G N, GYFTOPOULOS E P. Thermionic energy conversion[M]. Cambridge, Massachusetts, MIT Press, 1979.

[4] SEGEV G, ROSENWAKS Y, KRIBUS A, Efficiency of photon enhanced thermionic emission solar converters[J]. *Solar* Energy *Materials* & *Solar* Cells, 2012, **107**(1):125 - 130.

[5] VARPULA1 A, PRUNNILA M. Diffusion-emission theory of photon enhanced thermionic emission solar energy harvesters [J]. *Journal of Applied Physics*, 2012, **112**(044506): 1-5.

[6] RADZIEMSKA E. Thermal performance of Si and GaAs based solar cells and modules: a review[J]. *Progress in Energy and Combustion Science*, 2003, **29**(1): 407-424.

[7] YUAN Ji-ren, HONG Wen-qin, DENG Xin-hua. Influence of nickel impurity the performance of GaAs solar cells with impurity photovoltaic effect[J]. *Acta Photonica Sinica*, 2012, **41**(10): 1167-1170.

[8] MARTIN A, KEITH E, YOSHIHIRO H, *et al*. Solar cell efficiency tables (version 39)[J]. *Progress in Photovoltaics: Research and Applications*, 2012, **20**(1): 12-20.

[9] ORTIZ E, REY-STOLLE I, DIAZ V, *et al*. A GaAs solar cell with an efficiency of 26.2% at 1000 suns and 25.0% at 2000 suns[J]. *Electron Devices, IEEE Transactions on*, 2001, **48** (5): 840-844.

[10] NIU Jun, ZHANG Yi-jun, CHANG Ben-kang, *et al*. Influence of exponential doping structure on the performance of GaAs photocathodes[J]. *Applied Optics*, 2009, **48**(29): 5445-5450.

[11] DU Yu-jie, DU Xiao-qing, CHANG Ben-kang, *et al*. Spectral response performance of transmisson-mode GaAs photocathode in activation[J]. *Acta Photonica Sinica*, 2005, **34**(12): 1792-1794.

[12] LI Bao-xia, WANG Tao, LI Xiao-ting. Heavy carbon doping of GaAs by metalorganic chemical vapor deposition[J]. *Acta Photonica Sinica*, 2003, **32**(2): 249-252.

[13] ZOU Ji-ju, GAO Pin, YANG Zhi, *et al*. Influence of active-layer thickness on reflection-mode GaAs photocathode[J]. *Acta Photonica Sinica*, 2008, **37**(6): 1112-1115.

[14] GAO Fei, GUO Hui, HU Cang-lu, *et al*. Electrostatic bonding of GaAs photocathode materials to glass[J]. *Acta Photonica Sinica*, 2008, **37**(8): 1549-1552.

[15] CHENG Liang, QIAN Yun-sheng, CHANG Ben-kang. Reflection on surface photovoltage spectroscopy for transmission-mode GaAs photocathodes of different active layer thickness[J]. *Acta Photonica Sinica*, 2011, **40**(7): 1008-1012.

[16] ZHU Y M, UNUMA T, SHIBATA K, *et al*. Power dissipation spectra and terahertz intervalley transfer gain in bulk GaAs under high electric fields[J]. *Applied Physics Letters*, 2008, **93**(1): 232102.

[17] ZHU Y M, UNUMA T, SHIBATA K, *et al*. Femtosecond acceleration of electrons under very high electric fields in bulk GaAs investigated by time-domain terahertz spectroscopy[J]. *Applied Physics Letters*, 2008, **93**(1): 042116.

[18] PENG Y, WEN Y, ZHANG D S, *et al*. The optimal relation between laser power and pulse number for the fabrication of surface-microstructured silicon[J]. *Applied Optics*, 2011, **50**(1): 4765.

[19] PENG Y, ZHANG D S, CHEN H Y, *et al*. Differences in the evolution of surface-microstructured silicon fabricated by femtosecond laser pulses with different wavelength[J]. *Applied Optics*, 2012, **51**(1): 635.

[20] PENG Yan, CHEN Hong-yan, ZHU Cheng-gang, *et al*. The effect of laser wavelength on the formation of surface-microstructured silicon[J]. *Materials Letters*, 2012, **83**(1): 127.